IC/88/151

INTERNATIONAL CENTRE FOR THEORETICAL PHYSICS

STANDING NON-DISSIPATIVE SHOCKS
IN BLACK HOLE ACCRETION AND WINDS

Sandip K. Chakrabarti

INTERNATIONAL ATOMIC ENERGY AGENCY

UNITED NATIONS EDUCATIONAL, SCIENTIFIC AND CULTURAL ORGANIZATION

International Atomic Energy Agency
and
United Nations Educational Scientific and Cultural Organization

INTERNATIONAL CENTRE FOR THEORETICAL PHYSICS

STANDING NON-DISSIPATIVE SHOCKS IN BLACK HOLE ACCRETION AND WINDS *

Sandip K. Chakrabarti
International Centre for Theoretical Physics, Trieste, Italy.

ABSTRACT

We present all non-dissipative shock solutions for stationary, axially symmetric and rotating adiabatic flows of small transverse thickness in black hole potential. We show that for a given initial and final states of the flow, there can be as many as four formal shock locations in both the accretion and the winds. Only two (three) of these locations are acceptable for accretion onto black holes (neutron stars) and three of these locations are acceptable for winds. We prove that the shock strength and the temperature jump have a lower limit which does not depend upon the parameters of the flow or the force field in which the flow moves and is only a function of the adiabatic index of flow.

MIRAMARE - TRIESTE
July 1988

* Submitted for publication.

1 INTRODUCTION

Study of shocks in astrophysical flows has been greatly intensified in recent years. Various authors including Tsinganos, Habbal and Rosner (1983), Chang and Ostriker (1985), Hawley, Smarr and Wilson (1985), Sawada, Matsuda and Hachisu (1986) and most recently Fukue (1987) constructed shock solutions either analytically or by numerical simulation. In this analysis, the shock solutions were produced on a case-by-case basis and no general dependence on the parameter space was studied. In the present paper we construct solutions in a more general framework. We classify all $non-dissipative$ shock solutions in accreting flows or winds in terms of the flow parameters, such as the accretion rate, energy density and the angular momentum. In these shocks the energy density of the fluid remains constant, throughout the flow, but the entropy changes at the shocks. In a second paper (Chakrabarti, 1988a) we study exactly the opposite case, namely the properties of the *dissipative* shocks which are isentropic. In a realistic astrophysical situation a shock would be a combination of these cases depending on the physical processes present at the shock. In a third paper we study another important type of shocks which are isothermal (Chakrabarti, in preparation, see also Chakrabarti 1988b). In these shocks both the energy and the entropy are lost in order that they may remain isothermal. This is possible, for example, when efficient cooling processes are present at the shock. An overview of these works is presented elsewhere (Abramowicz and Chakrabarti, 1988, hereafter referred to as Paper I).

2 Basic flow equations and the Shock conditions

In what follows, we assume non-dissipative, thin, rotating, adiabatic accretion and winds near a compact object. The equations of motion used are for a 1.5 Dimensional fluid as in

Paper I, in the sense that no restrictions are imposed while writing the radial equations but equations in the transverse direction are kept "half-dimensionally" correct: the vertical equilibrium in transverse direction is assumed, while the motion along that direction is neglected.

Our stationary model is described by the dimensionless equations of energy, angular momentum and mass conservation supplied by the transonic conditions at the critical points and the canonical Rankin-Hugoniot conditions at the shock. We assume the Newtonian model for the central compact object (black hole or neutron star) given in terms of the Paczyński and Wiita (1980) potential. We also assume a polytropic equation of state for the accreted matter, $p = K\rho^{\gamma}$, where, p and ρ are the isotropic pressure and the matter density respectively, γ is the adiabatic index (assumed in this paper to be constant throughout the flow) and K is related to the specific entropy of the flow s: $s = const$ implies $K = const$. We assume that entropy, and thus K can vary only at the shock. As there is no dissipation in the flow, the specific angular momentum λ is constant everywhere.

The dimensionless energy conservation law can be written as

$$\mathcal{E} = \frac{\vartheta^2}{2} + \frac{a^2}{\gamma - 1} + \frac{\lambda^2}{2x^2} + g(x) \tag{1}$$

Here $g(x)$ is the radial force potential, which in the pseudo-Newtonian model takes the form: $g(x) = -1/2(x-1)$. Here, ϑ and a are the non-dimensional radial and sound velocities measured in units of velocity of light c, x is non-dimensional radial distance measured in units of the Schwarzschild radius $r_g = \frac{2GM}{c^2}$, M being the mass of the hole and G being the gravitational constant. Apart from a geometric factor the mass conservation equation is given by

$$\dot{M} = \vartheta \rho x h \tag{2}$$

where h is the thickness of the flow at radial co-ordinate x. We assume vertical equilibrium in the flow and h in our model is given by

$$h = ax^{1/2}(x-1). \tag{3}$$

Just for comparison, the conical flow is described by assuming $h \sim x$. It is useful to write the mass conservation equation in terms of ϑ and a in the following way,

$$\dot{M} = \vartheta a^q x^{3/2}(x-1) \quad , \tag{4}$$

where $q = \frac{\gamma+1}{\gamma-1}$. $\dot{M} = \dot{M}K^n$ does not remain constant at the shock because of the generation of entropy.

The shock conditions which we employ here are the following (subscripts '-' and '+' refer to quantities before and after the shock): The energy conservation equation,

$$\mathcal{E}_+ = \mathcal{E}_-, \tag{5a}$$

the pressure balance condition,

$$P_+ + \rho_+ \vartheta_+^2 = P_- + \rho_- \vartheta_-^2 \tag{5b}$$

and the baryon number conservation equation,

$$\dot{M}_+ = \dot{M}_- \tag{5c}$$

In order to have shocks the flow must be supersonic, i.e., the stationary flow must pass through a sonic point. The sonic point conditions are derived in the following way (see for example, Fukue 1982, Chakrabarti 1986, Paper I): differentiate the energy and mass conservation equations (eqns. 1-2) and substitute da/dx from one into the other to obtain,

$$\frac{d\vartheta}{dx}\left(\vartheta - \frac{2a^2}{(\gamma+1)\vartheta}\right) = \frac{2a^2}{(\gamma+1)}\frac{dlnf}{dx} - \frac{dG}{dx} \tag{6}$$

where, $G(x) = \frac{\lambda^2}{2x^2} - \frac{1}{2(x-1)}$ is the effective potential. The left-hand side and the right-hand side vanish simultaneously at the critical points, where the velocity ϑ_c is related to the sound speed a_c by,

$$v_c^2(x_c) = \frac{2}{(\gamma+1)} a_c^2(x_c). \tag{7a}$$

The vanishing of the right-hand side gives the sound at the outer critical point as,

$$a_c^2(x_c) = \frac{(\gamma+1)(x-1)}{x^2} \frac{(\lambda_k^2 - \lambda^2)}{(5x-3)}. \tag{7b}$$

Eqns. (1), (4), (5a-c), (7ab) are simultaneously solved in the next section to obtain full shock solution.

3 Mach number Relation at the Shock

To classify the shock solutions in terms of the flow parameters, it is useful to look for some invariants through the shock since these are easier to deal with. For this we re-write the energy conservation eqn. (5a), the mass conservation eqn. (4) and the pressure balance equation (5b) in terms of the Mach number $M = \frac{\vartheta}{a}$ of the flow,

$$\frac{1}{2} M_+^2 a_+^2 + \frac{a_+^2}{\gamma-1} = \frac{1}{2} M_-^2 a_-^2 + \frac{a_-^2}{\gamma-1} \tag{8a}$$

$$\dot{M}_+ = M_+ a_+^{\nu} f(x_s) \tag{8b}$$

$$\dot{M}_- = M_- a_-^{\nu} f(x_s) \tag{8c}$$

and

$$\frac{a_+^{\nu}}{\dot{M}_+}(1+\gamma M_+^2) = \frac{a_-^{\nu}}{\dot{M}_-}(1+\gamma M_-^2) \tag{8d}$$

where, $\nu = \frac{2\gamma}{\gamma-1}$ and x_s is the location of the shock. The true definition of the Mach number in our model of thin flow with the vertical equilibrium is $M = \frac{\sqrt{\gamma+1}\vartheta}{a}$ (*cf.* eqn. (7)) since a small acoustic perturbation can be shown to propagate with velocities $a\sqrt{\frac{2}{\gamma+1}} \pm \vartheta$. However, since none of the following results depend on the re-definition of the Mach number we shall continue to use $M = \frac{\vartheta}{a}$ for simplicity. From eqns. (8b-d), one obtains the following equation relating the Mach numbers of the flow at the shock,

$$\frac{1}{M_+} + \gamma M_+ = \frac{1}{M_-} + \gamma M_- = 2C, \quad \text{(say)} \tag{9}$$

The constant C as defined above is invariant across the shock. A number of important results can be derived from this relation. The Mach number of the flow just before and after the shock can be written down in terms of C as,

$$M_{\mp} = \frac{C \pm \sqrt{C^2 - \gamma}}{\gamma}. \tag{10a}$$

The product of which is

$$M_+ M_- = \frac{1}{\gamma}. \tag{10b}$$

Since $\gamma \geq 1$ for adiabatic flows, it is immediately clear that the shock strength $\Sigma = \frac{M_-}{M_+}$ cannot be arbitrarily close to unity except for isothermal flows. At the critical point Mach number is $M_{crit} = \sqrt{\frac{2}{\gamma+1}}$ and the shock strength should be at least $\Sigma = \frac{2\gamma}{\gamma+1}$. A more rigorous limit is provided below. The ratio of the flow temperatures is given by the energy balance equation,

$$\frac{T_-}{T_+} = (\frac{a_-}{a_+})^2 = \frac{(\gamma-1)M_+^2 + 2}{(\gamma-1)M_-^2 + 2} \tag{11}$$

For extremely weak shocks the entropy changes infinitesimally, i.e, $\dot{M}_- = \dot{M}_+$. This condition on eqns. (8b,c) along with the one given above (eqn. 11) gives (Chakrabarti, 1988c)

$$\Sigma = \frac{M_-}{M_+} = \left[\frac{(\gamma-1)M^2_- + 2}{(\gamma-1)M^2_+ + 2}\right]^{\frac{\gamma}{\gamma-1}} \tag{12}$$

This relation and eqn. (10b) determines the Mach numbers uniquely at the weak shock transition as a function of the adiabatic index γ. Note that $\Sigma = 1$ for isothermal flows. One derives absolute lower limit of the shock strength from this result. Fig. 1 shows the ratio of the temperatures and the shock strength Σ obtained from above relation. As is clear, apart from its dependence on γ the limit is independent of any of the flow parameters or the force field in which the flow moves. There is also an upper limit of the shock strength for black hole accretion. However, this limit depends on the flow parameters, and will be discussed later.

4 Black Hole Accretion and Winds in 1.5D Model

In what follows we assume that the adiabatic index $\gamma = 4/3$ for the flow. We shall also use the term 'accretion rate' for $\dot{M}$ although it increases at the shock due to generation of entropy. Fig. 2 shows the variation of the energy of the flow as a function of the location of the critical points for various angular momenta. Since both the energy and the angular momentum remain constant throughout the flow (even when the shock is present), the intersection of a horizontal line and a curve gives the critical point locations through which flow must pass. It is clear that angular momentum below $\lambda = 1.491$ (dashed curve) there is only one critical point in the flow and therefore shocks are not possible. In general, when two critical points are present, the values of $\dot{M}$ are different at these points, i.e, $\dot{M}_- \neq \dot{M}_+$ except for a very special point for each angular momentum, when both are same (locus of these points is BD in Fig. 3 below). The dashed curve ABC is the locus of the extrema. Fig. 3 shows how this curve looks like when mapped onto $log(\lambda^2)$ $vs.$ $\dot{M}$ plane. For a given angular momentum $\lambda_{min} \leq \lambda \leq \lambda_{max}$, there are two accretion rates $\dot{M}_{min}$ and $\dot{M}_{max}$ (lying on branches AB and BC respectively) such that flow with $\dot{M} > \dot{M}_{max}$ passes through only the inner critical point (region I) and flow with $\dot{M} < \dot{M}_{min}$ passes through only the outer critical point (region O). The flow has only one critical point in these two regions. We also draw a curve ED which corresponds to $\mathcal{E} = 0$. The flow in region AED (region B) is bound in the sense that although winds with parameters from this region can formally pass through the innermost critical point, they cannot escape to a large distance. In regions bounded by BDC (region W) and by BED (region A) accretion flow is always transcritical and *formally* passes through either the innermost critical point or the outermost critical point depending on the accretion rate $\dot{M}$ (for a given energy). In region W, flow with lower accretion rate passes through the innermost critical point whereas in region A flow with lower accretion rate passes through the outermost critical point. Therefore,

provided all the shock conditions are satisfied, winds in region W and accretion in region A may have shocks. Flows in these two regions have three critical points, two are 'X' type (*i.e.*, saddle points) and the central one is 'O' type (*i.e.*, a center point). For the purpose of future reference, we give the coordinates $(\lambda, \dot{M})$ of the most important points of this parameter space: $A = (1.79, 0.0)$, $B = (1.491, 2.7288)$, $E = (1.61, 0.88)$, $D = (2.0, 0.0)$. In the next section, we describe in detail the parameter space available for stationary solutions (with or without shocks) for accretion and for winds.

5 Examples and full classification of non-dissipative shock solutions

5.1 Accretion Flows

In a stationary black hole accretion with shocks, the flow must pass through the outer critical point, possibly pass through a shock and finally must pass through the inner critical point. In a neutron star accretion the flow need not pass through the inner critical point and if it does it must pass through another shock before touching the star surface. In Fig. 4, we redraw part of Fig. 3 inside a dashed box with subdivisions of region A (between curves B_1D_1 and B_2A_2). The region A_1 between curves S_1S_2 and B_1D_1 contains parameters which produces non-dissipative shocks in accretion flows. All the shock conditions are satisfied formally at four places, two in between the two 'X' type critical points, and two outside them. The post shock parameters lie in region A_2 between curves F_1F_2 and B_1D_1. Points S_1 and F_1 merge at $\lambda \approx 1.64$. Below this angular momentum, shock conditions are satisfied outside the critical points. No shock is possible for winds with parameters below the midline B_1D_1. The region A_3 between S_1S_2 and A_2B_2 has all the properties of region A_1 except that the flow may have formal shock locations only outside the critical points. Since these 'shock' are of limited importance, we shall not study them further.

A useful way to visualize whether and where shocks should form would be to check if the Mach number relation (9) is satisfied at any point in the flow. This is done by plotting contours of constant $\dot{M}_-$ and $\dot{M}_+$ for a given energy $\mathcal{E}$ and angular momentum λ and see if they intersect. An example of such a plot is shown in Fig. 5a for flow parameters ($\mathcal{E} = 0.48e-02$, $\dot{M}_- = 0.5e-05, \lambda = 1.7$) corresponding to region A_1. The four possible shock locations denoted by s_{ii}, s_i, s_o, and s_{oo} are shown where all the shock conditions are simultaneously satisfied. (Since we are interested in the nature of intersections, no attempt is made to describe the figures in detail.) In all these cases, the initial and the final states of matter are exactly the same. In the case of accretion onto black holes for non dissipative flows which are subsonic at large distance and supersonic on the horizon, s_i and s_o are the only two possibilities for shocks. However, for accretion onto neutron stars, s_{ii} is also a possibility. This agrees with the findings of Fukue (1987) that neutron star accretion may have three shock locations. The parameters for the upper limit of the shock strength is obtained from the condition of $s_i = s_o$ and represents the curve S_1S_2 in Fig. 4. Fig. 5b shows the accretion with flow parameter with low angular momentum. The parameters are $\mathcal{E} = 0.82e-02, \dot{M}_- = 1.05e-05, \lambda = 1.625$. Clearly, there are only two s_{ii} and s_{oo} shock locations. Fig. 6 shows the contours of constant accretion rate for parameters of the flow with which Fig. 5a was drawn. The possible locations of the shocks are also indicated by short vertical lines.

Fig. 7 shows the $\dot{M}$-$\mathcal{E}$ plot for $\lambda = 1.7$. A typical shock transition in accretion is shown by the solid horizontal line s_1s_2. The whole parameter space division in terms of the energy of the flow is also shown in this figure. For $\mathcal{E} \geq \mathcal{E}_i$ there is only one critical point and no shock is possible. For $\mathcal{E}_m \leq \mathcal{E} \leq \mathcal{E}_i$ (see inset) the accretion rate $\dot{M}_- \geq \dot{M}_+$ and shock is not possible either since the entropy will *decrease* in the

process. For $\mathcal{E}_s \leq \mathcal{E} \leq \mathcal{E}_m$ shocks form with the change of entropy calculated from the two intersection points such as s_1 and s_2. For $\mathcal{E}_o \leq \mathcal{E} \leq \mathcal{E}_s$ the pressure balance condition is satisfied only outside the sonic points. Shock is possible only for neutron star accretion. For $\mathcal{E} < \mathcal{E}_s$ flow passes through only the outer critical point.

5.2 Wind Flows

We now briefly repeat a similar analysis for wind flows. In this case the flow must pass through the inner critical point, and after possible shocks must pass through the outer critical point. However, if the outer boundary condition is subsonic, the flow need not pass through the outer critical point, or, if it does, must through another shock. In Fig. 8 we re-draw the dashed box of Fig. 3, this time dividing the region W into regions appropriate for shock formation in wind flows. Briefly, in this case, the flow with parameter in region W_1 bounded by the curves S_1S_2 and the midline B_1D_1 passes through shock and the post shock parameters lie in the region W_2 bounded by the curves F_1F_2 and the midline B_1D_1. For flow parameters beyond F_1F_2 the shocks inside the two critical points are not possible. In Fig. 7, we show a typical shock transition by a dashed horizontal line, w_1w_2. Just as $\mathcal{E}_s$ defines the boundary of shocked accretion, $\mathcal{E}_w$ represents the boundary of the shocked winds.

Figs. 9a-9b show the contours of constant accretion rates in the C-x_s plane for two typical flow parameters, one from region W_1 and the other with lower angular momentum. The former ($\mathcal{E} = 0.55e-02$, $\dot{M}_- = 0.53e-05, \lambda = 1.7$) shows that like the case of accretion, there could be as many as four possible locations where all the shock conditions are satisfied. The innermost 'shock' is not possible for winds. But one of the three others could be a possibility depending upon the boundary conditions. Fig. 9b shows that only s_{ii} and s_{oo} are present when the angular momentum chosen is low

$\lambda < 1.64$. The flow parameters are $\mathcal{E} = 0.86e-02$, $\dot{M}_{-} = 1.09e-05, \lambda = 1.625$. Fig. 10 shows the contours of constant accretion rates corresponding to the parameters of Fig. 9a. The locations of the shocks are shown by short vertical lines.

6 Implications of multiplicity of shock locations and Concluding remarks

The variation of the shock locations as a function of the flow parameters is shown in Figs. 11(a-d) for both the accretion (solid) and winds (dashed). Fig. 12 shows the change in the strength of the shock Σ. Notice that for all angular momentum and energy the shock strength $\Sigma \geq 2.852$, a number obtained from equations (10b and 12, see also Fig. 1). The behaviours of s_{ii} and s_o are similar but opposite to the behaviours of the shocks s_i and s_{oo}. The whole range of energy in which s_{oo} and s_{ii} may form is much higher (the whole region A and W) than what is shown in these Figures although for s_o and s_i it is complete. In reality, for black hole accretion it is not straightforward to judge which one of s_o and s_i the nature would choose, a question raised by Fukue (1987). It is also clear from Figs. (5ab and 9ab) above that if a small dissipation is allowed at the shock, the number of intersections, should still remain the same. However, in future (Chakrabarti, in preparation) in our discussion of the isothermal shocks, we shall show that the location of the shock becomes unique in most of the parameter space. The answer of uniqueness may therefore depend upon the ability of the flow to dissipate, an answer suggested in Paper I. If the flow itself has any dissipation even away from the shock it may also lift the degeneracy. We hope to clear these issues in future.

ACKNOWLEDGMENTS

The author would like to thank Professor Abdus Salam, the International Atomic Energy Agency and UNESCO for hospitality at the International Centre for Theoretical Physics, Trieste, Italy.

REFERENCES

Abramowicz, M. A. and Chakrabarti, S. K. 1988, *Ap. J.* (Submitted).

Chakrabarti, S.K. 1986, *Ap. J.*, **303**, 582.

Chakrabarti, S.K. 1988a, *ICTP*, Trieste, Preprint No. IC/88/153.

Chakrabarti, S.K. 1988b, *ICTP*, Trieste, Preprint No. IC/88/152.

Chakrabarti, S.K. 1988c, *ICTP*, Trieste, Preprint No. IC/88/150.

Chang, K. M., and Ostriker, J. P. 1985, *Ap. J.*, **288**, 428.

Fukue, J. 1982, *Publ. Astron. Soc. Japan*, **34**, 163.

Fukue, J. 1987, *Publ. Astron. Soc. Japan*, **39**, 309.

Habbal, S. R. and Tsinganos, K. 1983, *J. Geophys. Res.*,**88**, 1965.

Hawley, J.W., Smarr, L. and Wilson, J. 1985, *Ap. J.*, **277**, 296.

Paczyński, B and Wiita, P. J. 1980, *Astr. Ap.*, **88**, 23.

Sawada, K., Matsuda, T. and Hachisu, I. 1986, *M.N.R.A.S.*, **219**, 75.

Tsinganos, K., Habbal, S.R., and Rosner, R. 1983, *NASA STIB Conf. Publ.* **2280**.

FIGURE CAPTIONS

Fig. 1: Lower limit of the temperature jump $\frac{T_+}{T_-}$ (dashed line) and the shock strength $\Sigma = \frac{M_-}{M_+}$ (solid line) are plotted as a function of the adiabatic index γ. The ratios are independent of the flow parameters and goes to unity only for isothermal flows.

Fig. 2: Variation of $\mathcal{E}$ with the location of the critical points for a set of angular momentum λ: from the top curve to the bottom $\lambda = 1.4, 1.491, 1.6, 1.65, 1.7, 1.75, 1.8$ respectively. Flow with $\lambda < 1.491$ does not have more than one critical point. The long dashed curve ABC is the locus of the extrema of these set and is mapped in $\lambda - \dot{M}$ plane in Fig. 3.

Fig. 3: Division of the parameter space corresponding to different types of flow. Curve ABC is the locus of the extrema of the curves drawn in Fig. 2. Curve BD is the locus of accretion rates for which both the energy and the angular momentum of the fluid at the inner and outer critical points are the same. In region AED the energy of the flow passing through the inner critical point is negative. The dashed boxed part is discussed in detail in Fig. 4.

Fig. 4: The dashed box of Fig. 3 is re-drawn with further subdivisions according to whether or not an accreting flow must pass through a shock. Accretion flow with parameter from region A_1 between curves S_1S_2 and B_1D_1 has four locations at which shock conditions are satisfied, and the post shock parameters lie in the region A_2 between curves F_1F_2 and B_1D_1. Flow with parameter from region A_3 between S_1S_2 and A_2B_2 has two locations outside the 'X' type critical points in which shock conditions are satisfied. The dashed vertical line corresponds to $\lambda = 1.7$.

Fig. 5a: Example of contours of constant $\dot{M}_-$ and $\dot{M}_+$ satisfying shock conditions in accretions for a given energy $\mathcal{E}$ and angular momentum λ in the $C - x_s$ plane. The points of intersections s_{ii}, s_i, s_o, s_{oo} are the possible locations of the shock. The parameters used in this particular plot are $\mathcal{E} = 0.48e-02$, $\dot{M}_- = 0.5e-05, \lambda = 1.7$. Here c_1 and c_2 represent the locations of the critical points.

Fig. 5b: Same as Fig. 5a but for parameters $\mathcal{E} = 0.82e-02$, $\dot{M}_- = 1.05e-05, \lambda = 1.625$ which satisfy shock conditions only outside the critical point locations.

Fig. 6: Nature of accretion flow for parameters same as Fig. 5a. Along the abscissa is the logarithmic radial distance X and along the ordinate is the Mach number of the flow. At the sonic point, the Mach number is 0.93. The contours are of constant accretion rate $\dot{M}$. The shock locations are: $X_{s_1} = 2.095$, $X_{s_2} = 3.855$, $X_{s_3} = 18.2$, $X_{s_4} = 131.8$.

Fig. 7: Variation of energy of the flow with the accretion rate when the angular momentum is kept fixed and is equal to 1.7. The dashed box contains parameters important for shocks. This region is expanded and placed in the inset. See text for details of the different subdivisions in the energy scale.

Fig. 8: A figure similar to Fig. 4 is drawn for winds. Winds with parameter from region W_1 between curves S_1S_2 and B_1D_1 has four locations at which shock conditions are satisfied, and the post shock parameters lie in the region W_2 between curves F_1F_2 and B_1D_1. Flow with parameter from region W_3 beyond S_1S_2 has two locations outside the 'X' type critical points in which shock conditions are satisfied. The dashed vertical line coresponds to $\lambda = 1.7$.

Fig. 9a: Example of contours of constant $\dot{M}_-$ and $\dot{M}_+$ satisfying shock conditions in wind flows for a given energy $\mathcal{E}$ and angular momentum λ in the $C - x_s$ plane. The points of intersections s_{ii}, s_i, s_o, s_{oo} are the possible locations of the shock. The parameters used in this particular plot are $\mathcal{E} = 0.55e-02$, $\dot{M}_- = 0.53e-05, \lambda = 1.7$. Here c_1 and c_2 represent the locations of the critical points.

Fig. 9b: Same as Fig. 9a but for parameters $\mathcal{E} = 0.86e-02$, $\dot{M}_- = 1.09e-05, \lambda = 1.625$ which satisfy shock conditions only outside the critical point locations.

Fig. 10: Figure similar to 6 but for wind flows. Contours of constant accretion rate drawn for parameters of Fig. 9a. The shock locations are $X_{s_1} = 1.98$, $X_{s_2} = 5.33$, $X_{s_3} = 11.8$, $X_{s_4} = 116.9$.

Fig. 11(a-d): The variation of the location of the shocks in accretion (solid) and winds (dashed) as a function of $\mathcal{E}$ and λ. a) innermost shock location x_{ii}, b) inner shock location x_i, c)outer shock location x_o and d) the outermost shock location x_{oo}. At all these four locations the flow parameters change by the same amount. For Figs. 11b-c from right to left, pair wise, $\lambda = 1.65, 1.675, 1.7, 1.725, 1.75$. For Figs. 11a and 11d the rightmost pair is for $\lambda = 1.525$. λ increases by 0.025 for each pair leftwards.

Fig. 12: The variation of the strength of the shock in accretion (solid) and winds (dashed) as a function of $\mathcal{E}$ and λ. From the right to the left, pair-wise, $\lambda = 1.65, 1.675, 1.7, 1.725, 1.75$.

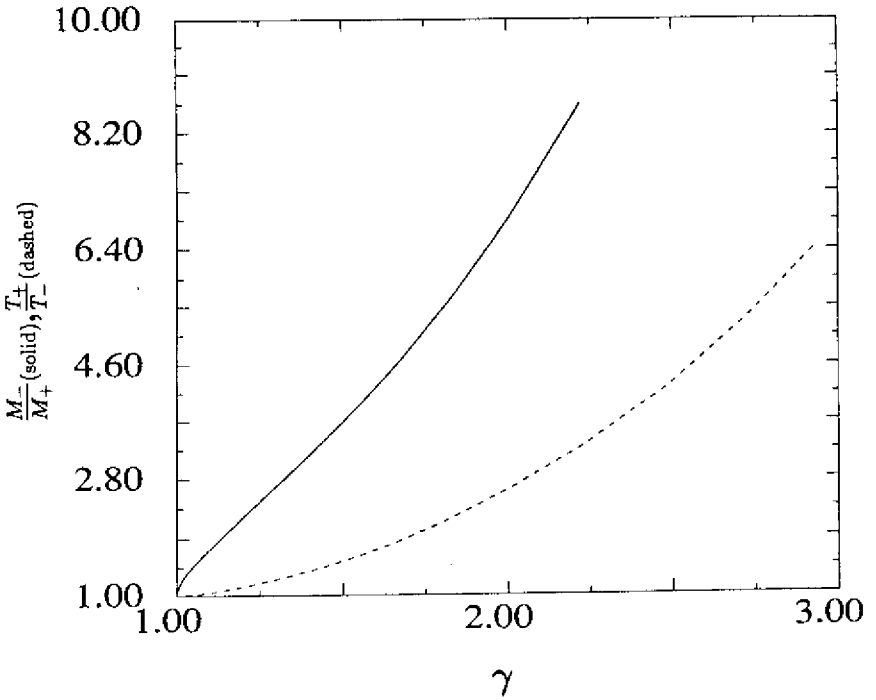
10.00
8.20
6.40
4.60
2.80
1.00
1.00
2.00
3.00
γ
$\frac{M_-}{M_+}$(solid), $\frac{T_+}{T_-}$(dashed)

Fig.1

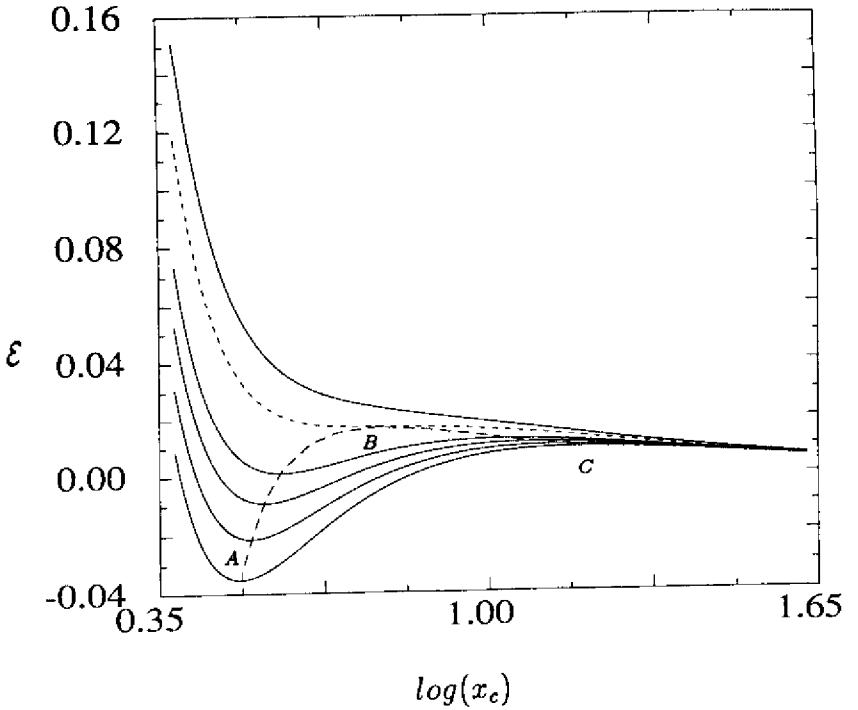
0.16
0.12
0.08
0.04
0.00
-0.04
0.35
1.00
1.65
ε
A
B
C
$log(x_c)$

Fig.2

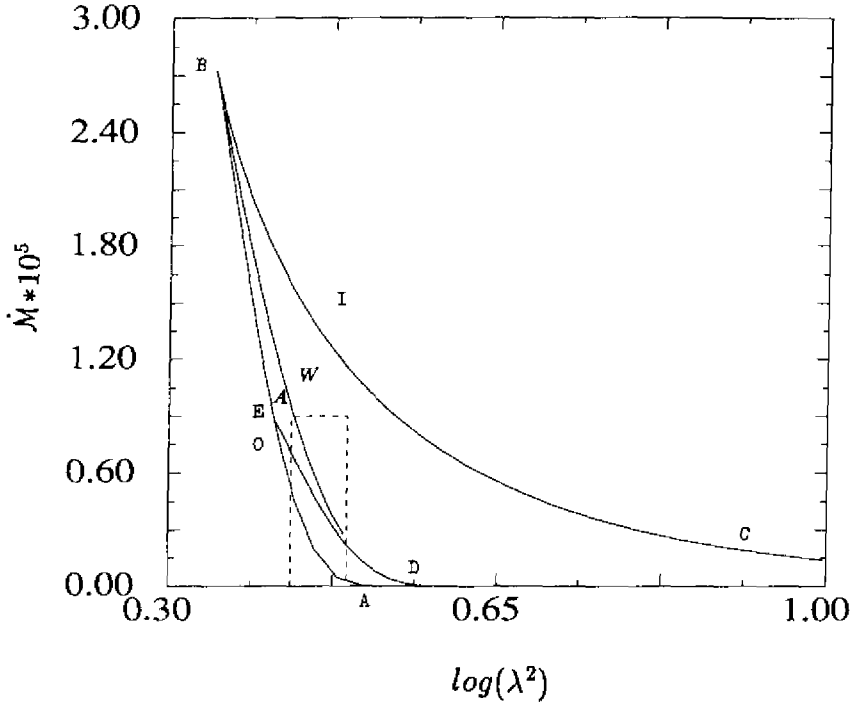
3.00
2.40
1.80
1.20
0.60
0.00
0.30
0.65
1.00
$\dot{M}*10^5$
$log(\lambda^2)$
B
I
W
A
E
O
C
D
A

Fig.3

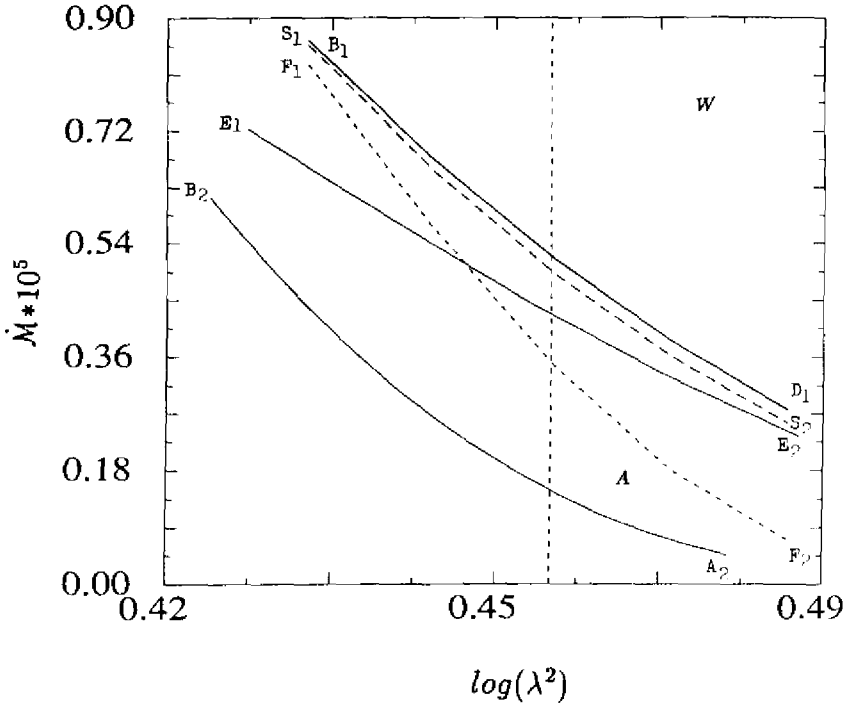
0.90
0.72
0.54
0.36
0.18
0.00
0.42
0.45
0.49
$\dot{M}*10^5$
$log(\lambda^2)$
S_1
B_1
F_1
W
E_1
B_2
D_1
S_2
E_2
A
A_2
F_2

Fig.4

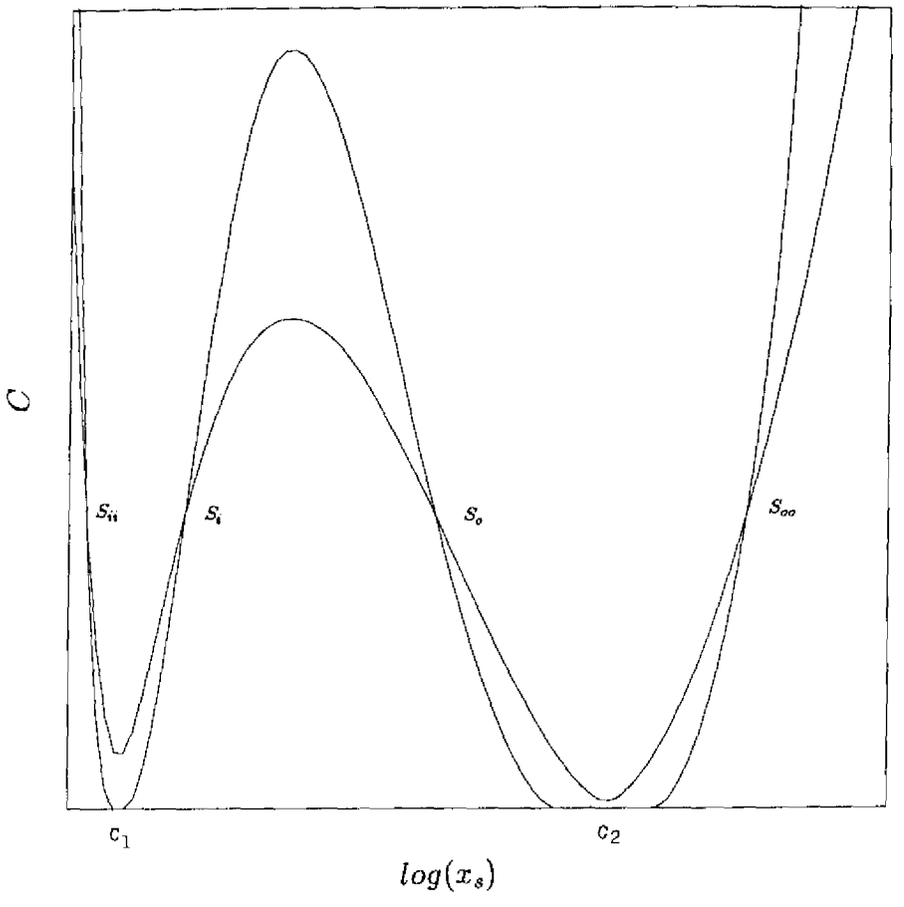

Fig.5a

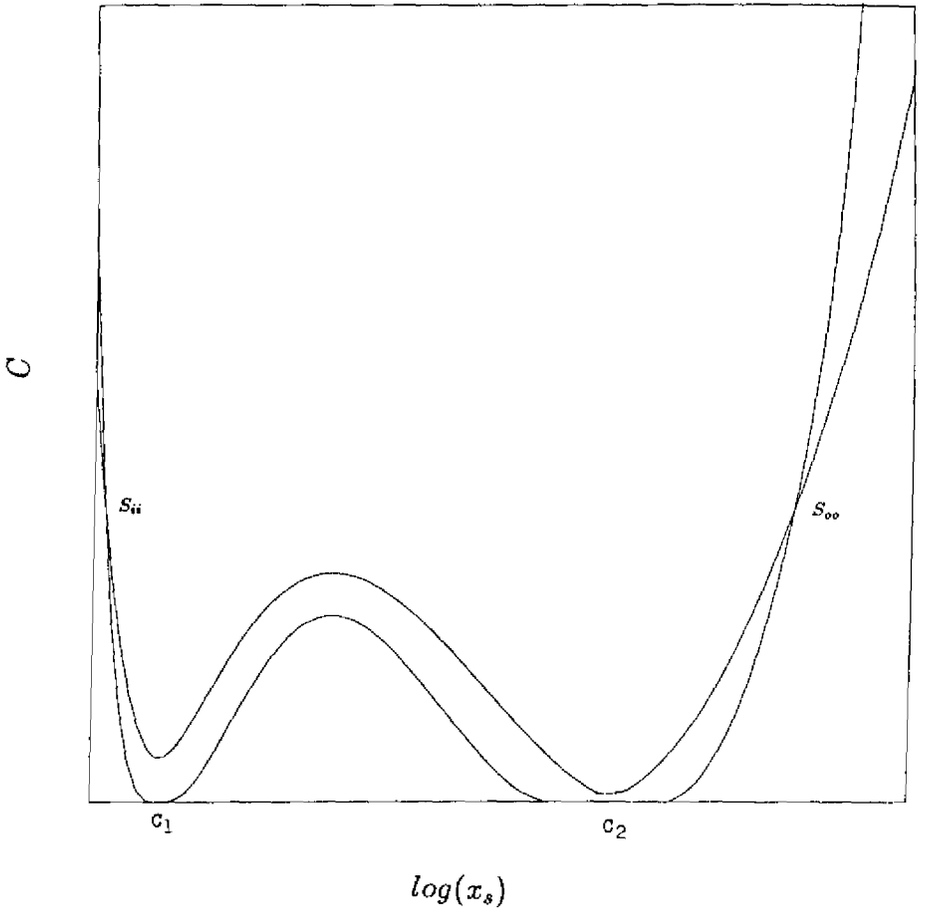

Fig.5b

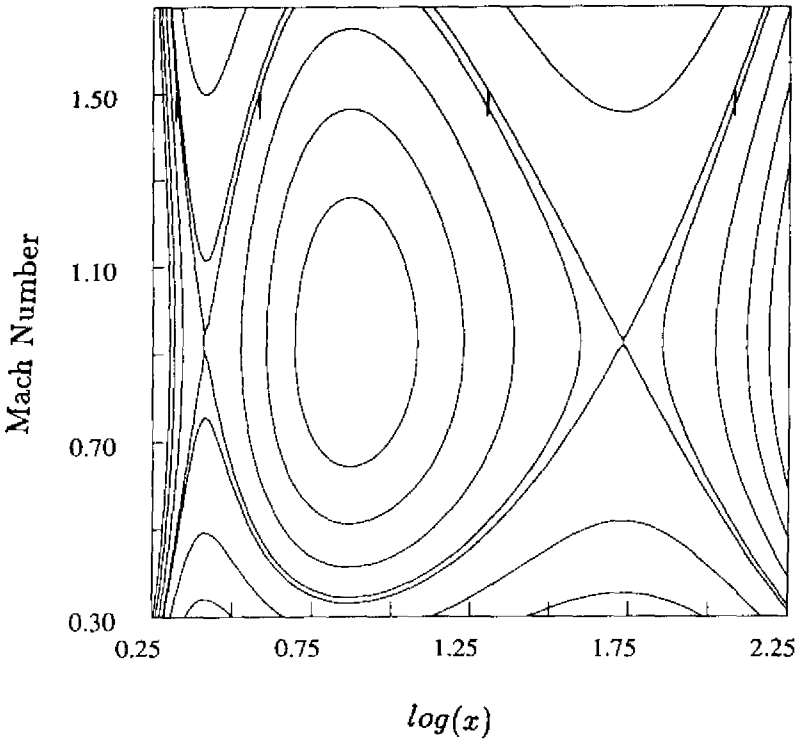
Mach Number
1.50
1.10
0.70
0.30
0.25
0.75
1.25
1.75
2.25
log(x)

Fig.6

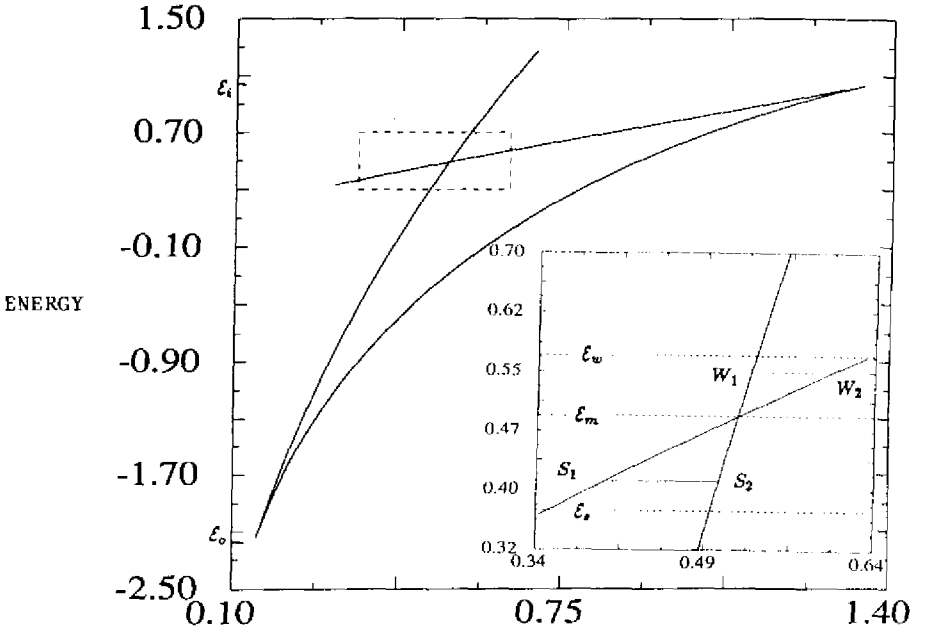
ENERGY
1.50
0.70
-0.10
-0.90
-1.70
-2.50
0.10
0.75
1.40
$\mathcal{E}_i$
$\mathcal{E}_o$
0.70
0.62
0.55
0.47
0.40
0.32
0.34
0.49
0.64
$\mathcal{E}_w$
$\mathcal{E}_m$
S_1
S_2
$\mathcal{E}_s$
W_1
W_2
ACCRETION RATE

Fig.7

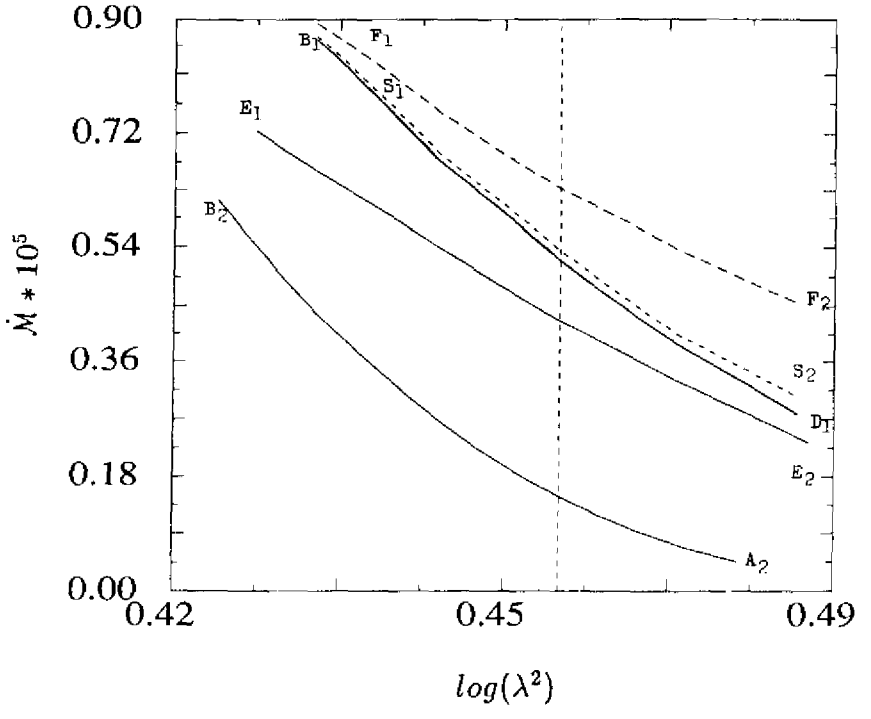
0.90
0.72
0.54
0.36
0.18
0.00
0.42
0.45
0.49
$\dot{M} * 10^5$
$log(\lambda^2)$
B_1
F_1
S_1
E_1
B_2
F_2
S_2
D_1
E_2
A_2

Fig.8

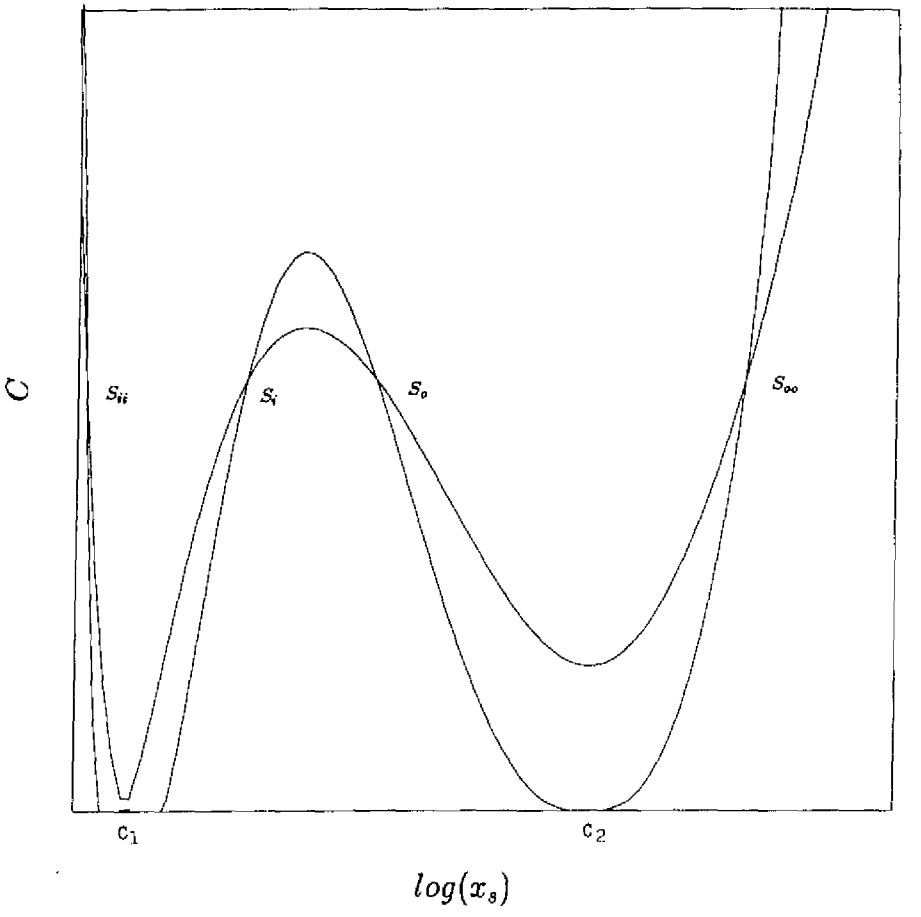
C
S_{ii}
S_i
S_o
S_{oo}
C_1
C_2
$log(x_s)$

Fig.9a

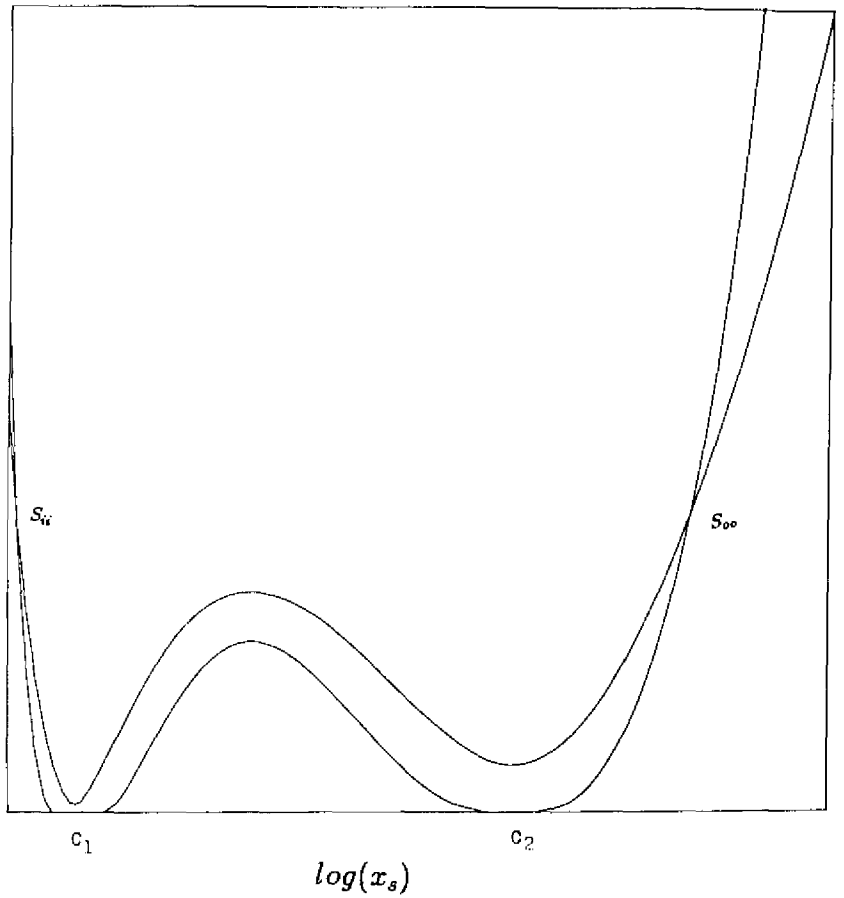
C
S_{ii}
S_{oo}
C_1
C_2
$log(x_s)$

Fig.9b

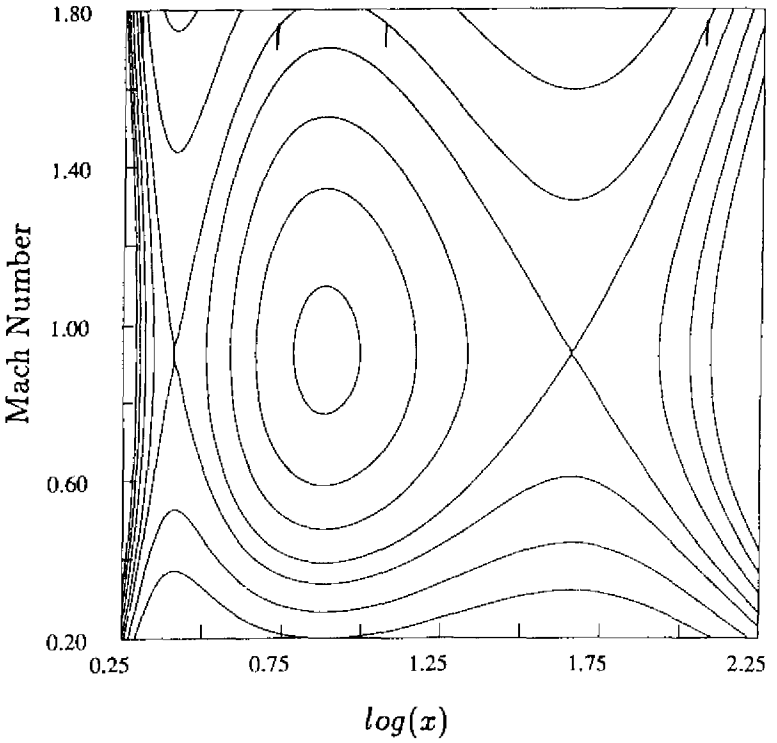
1.80
1.40
1.00
0.60
0.20
Mach Number
0.25
0.75
1.25
1.75
2.25
$log(x)$

Fig.10

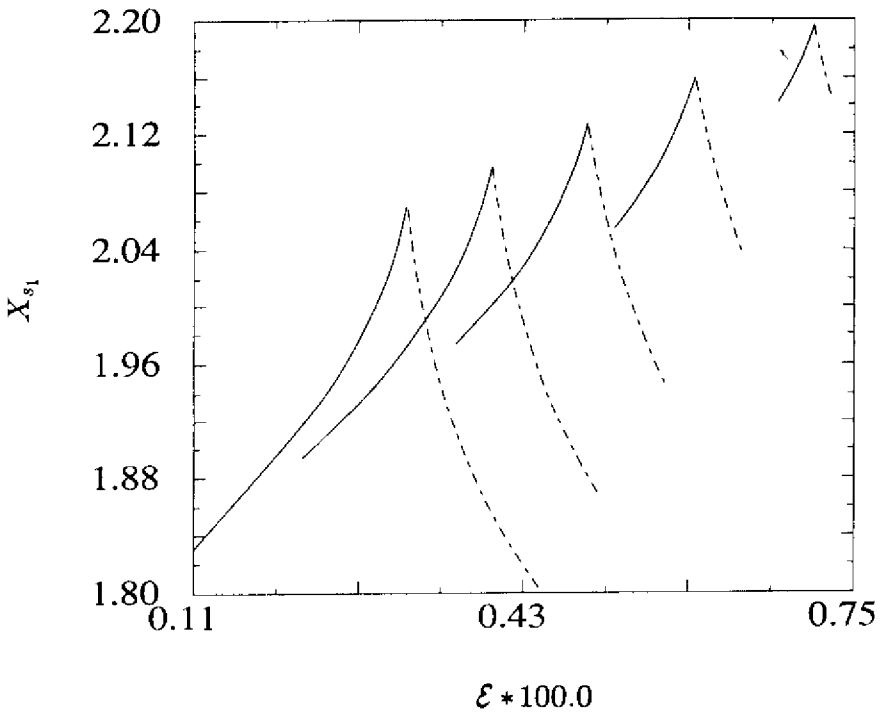

Fig.11a

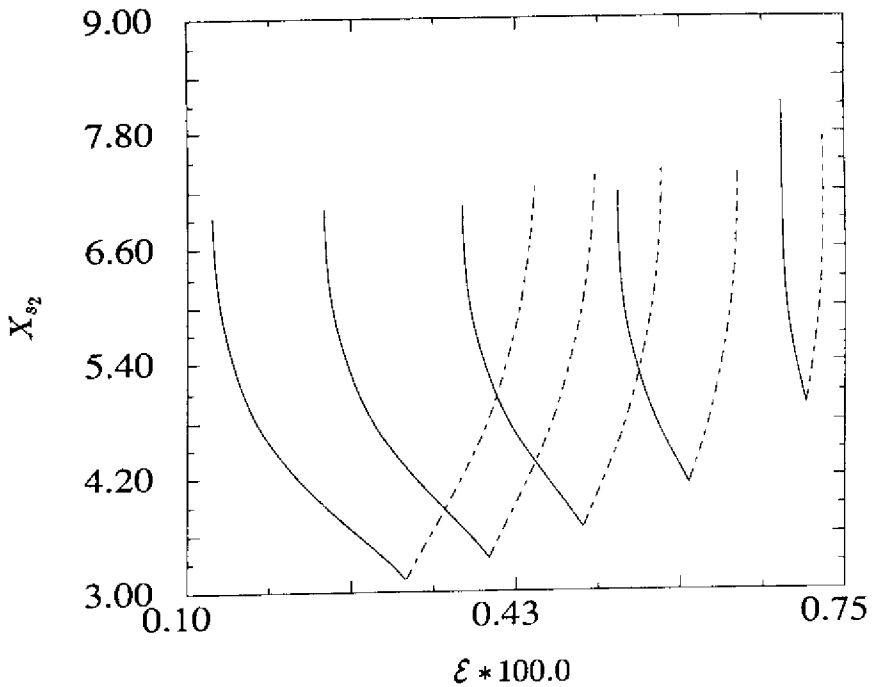

Fig.11b

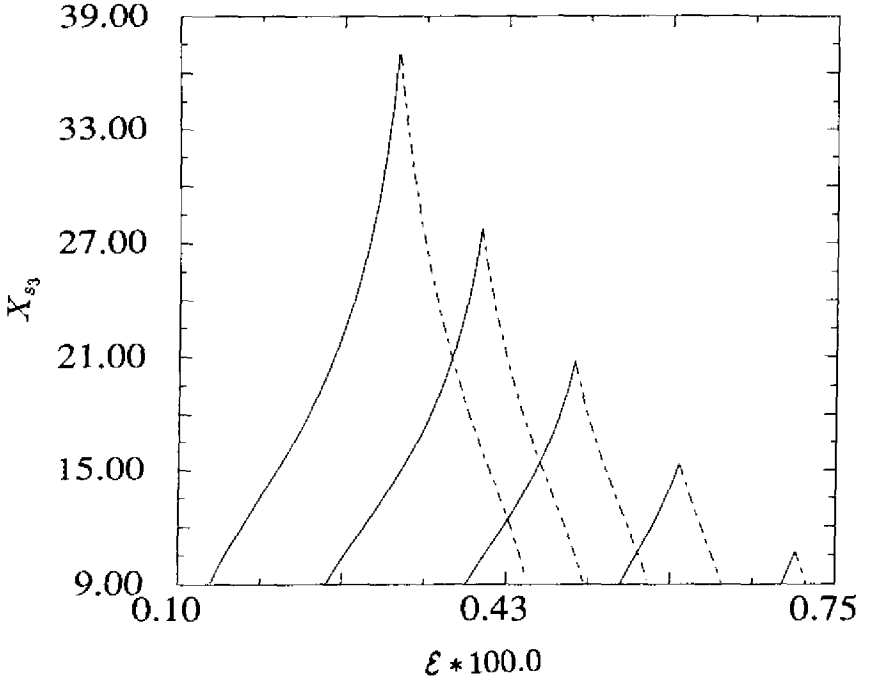

Fig.11c

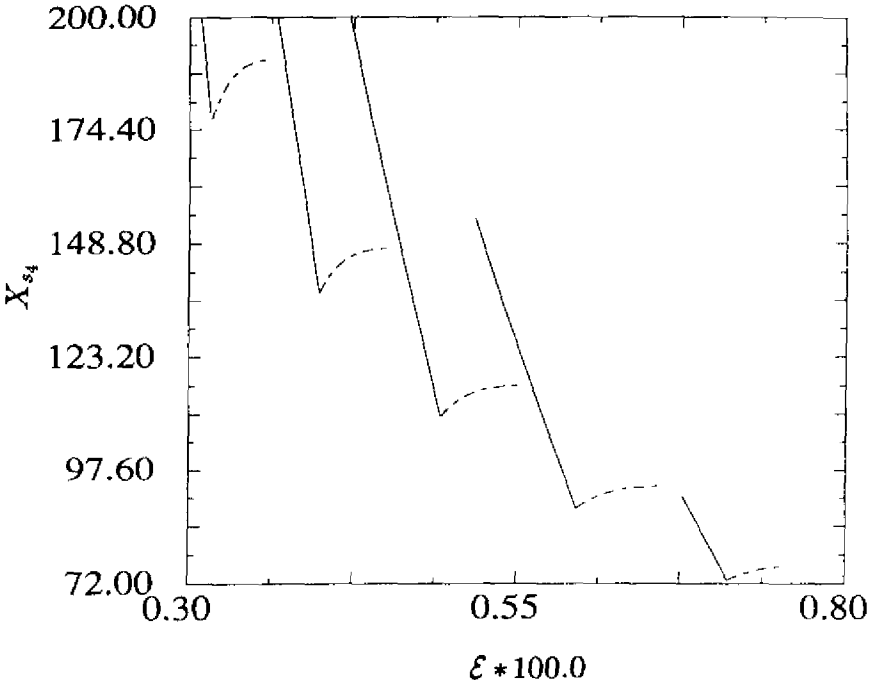

Fig.11d

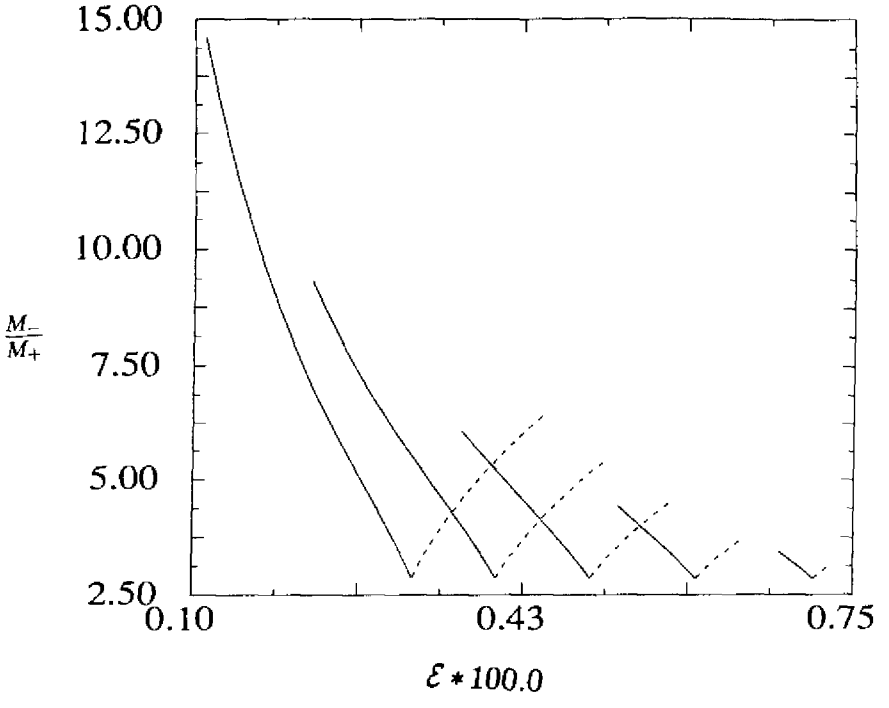

Fig.12

Stampato in proprio nella tipografia
del Centro Internazionale di Fisica Teorica